

Response Surface Methodology-based Optimization of Variable Compression Ratio Diesel Engine Characteristics with Jatropha Biodiesel

H. S. Anantha Padmanabha* and Dillip Kumar Mohanty

School of Mechanical Engineering, VIT-AP University, Amaravati - 522237, Andhra Pradesh, India;
pavanaputra304@gmail.com

Abstract

The use of biodiesels as a potential alternative to fossil fuels has significantly increased in the past few decades owing to their clean and renewable nature. The present work has considered jatropha oil as the feedstock for biodiesel due to its properties similar to that of petroleum diesel, large-scale availability, and improved engine characteristics. The brake thermal efficiency and brake-specific fuel consumption have been analyzed for estimating the engine performance while the emissions of hydrocarbon, carbon monoxide, and oxides of nitrogen have been considered for the exhaust emission. Further, the response surface methodology has been adopted for the optimization of the different engine characteristics. The response surface methodology has identified optimal engine characteristics of a variable ratio compression ignition engine for biodiesel with 10% jatropha oil methyl ester at 18:1 compression ratio and 50% engine load. The desired factor of 0.615 and inaccuracy less than 5% of the present analysis can be considered as suitable and acceptable for the optimal parameters.

Keywords: Engine Performance, Exhaust Emissions, Jatropha Biodiesel, Optimization, Response Surface Method, Variable Compression Ratio

1.0 Introduction

The world has been strangely utilizing energy in different forms for its regular pursuit, and thus the demand for energy has been slowly growing owing to obvious cases such as the expansion of novel technologies that are overly reliant on external energy sources, population growth, and so on^{1,2}. At the moment, energy is generally obtained from fossil sources³. Depending upon the existing profit among the world, they are expected to endure a few more years. However, because of global warming, they cause emissions like Hydrocarbons (HC), carbon dioxide (CO₂), and other hazardous gases, leading in environment vary and atmosphere damage. Although diesel fuel is generally used in transport, energy generation, agriculture, and

other industries, it emits considerable amounts of nitrogen oxides and particulate particles, which contribute pollution to the atmosphere⁴. It is common knowledge that non-renewable fossil fuels pose a potential hazard in the form of resource exhaustion⁵.

In view of the foregoing findings, there is a need to study unique and promising alternative fuel mixes that may be employed in diesel engine applications. The majority of studies have suggested that the use of renewable energy sources is required^{6,7}. The greater part of renewable fuels had been utilized as additives to diesel fuel in varying amounts to reduce exhaust emissions while without affecting engine performance. In this environment, biofuel has emerged as a well-liked option that is derived from both edible and non-edible

*Author for correspondence

raw materials found in environment⁸. However, in order to prevent a conflict between food and fuel, researchers have been evaluating non-edible basic materials⁹. Biodiesel is a biofuel that has qualities comparable to diesel fuel and is made from monoalkyl esters of long-chain fatty acids resulting from a variety of biological sources¹⁰. In agreement with earlier research, biofuel has been identified as one of the greatest options for meeting the world's energy need^{11,12}. Cottonseed oil is brought out from the cottonseeds once the lint has been separated.

Optimization analysis is crucial when contemplating new fuels for engines to prevent negative effects on engine performance. Particularly, performance and exhaust emissions are important elements to check in diesel engines. Abundant techniques like grey relation analysis, non-linear regression, response surface methodology, Taguchi technique, and Least-Squares Support Vector Machine (LSSVM) have been employed to optimize emission and performance parameters¹⁴⁻¹⁶. The response surface method is an eminent technique for probing the challenges involved in engineering-based modeling and response parameter optimization that is hampered by experiment factors^{17,18}. By reducing the number of experiments and creating an appropriate experiment matrix, RSM takes the least amount of time to finish the procedure compared with other optimization approaches like LSSVM and Taguchi^{19,20}. Numerous scholars discussed how the RSM optimization method was employed successfully in engines as input variables. Yatish *et al.*, investigated the use of *Bauhinia variegata* oil to optimize biogas production using the RSM technique. Additionally, different engine loads were tested to determine the performance of the engine and to determine the best biodiesel blend for a reduction of emissions, particularly HC and CO²¹. Sunil *et al.* examined the parameters of soybean biodiesel using response surface methodology. During the study, they achieved an R² value of 0.9918. The results indicated that the developed models precisely represented the described processes³⁸. Pitchaiah *et al.*, explored the enhancement of performance and energy assessment of diesel-Bael biodiesel when combined with the DMC additive by using RSM technology. The DMC additive demonstrated a beneficial effect in fine-tuning emissions and performance, thereby bolstering the utilization

of Bael biodiesel³⁹. Jatropha is a fast-growing plant that thrives even in challenging soil conditions so that feedstock is available abundantly for production of the biodiesel. Besides, the biodiesel produced from jatropha oil exhibits quite similar thermo-physical properties as that of petroleum diesel which justifies the jatropha oil be one of the most suitable biodiesel-producing elements. The novelty of this study lies in determining the optimized regions for speed, load, and injection timing based on engine responses. This allows for the identification of feasible parameters that enhance engine outcomes. The practical significance of this research is that it helps pinpoint specific input conditions that yield desired emission or performance results.

RSM seeks to establish a connection between a response and various influencing variables or factors using suitable experimental design and evaluation. Through RSM, multiple polynomial regression equations are employed to determine the functional association between these factors and the corresponding response values. This regression analysis helps in fine-tuning process parameters and forecasting response outcomes. Given that RSM can evaluate the impacts of numerous factors and their interrelationships on multiple response variables, it frequently finds application in diverse optimization situations¹⁵.

In this study, the blends 10, 20 and 30 % of methyl ester extracted from jatropha oil blended with diesel were used in variable compression ratio engine to evaluate the performance and emission characteristics at a constant speed with varying compression ratios from 16 to 18 and 50, 75 and 100 % of engine loads. More significantly, RSM was utilized to optimize the test diesel engine's operational parameters in an effort to identify the optimal engine emission and performance characteristics.

2.0 Methods

2.1 Biodiesel Preparation

In the presence of a catalyst, Jatropha oil undergoes a chemical reaction with an alcohol (methyl) to produce the methyl ester. A two-stage procedure is employed for jatropha oil transesterification. The esterification of methanol (99% pure) with sulfuric acid (98%) in a closed reactor vessel for one hour at 57°C is the first stage of

the acid-catalyzed process, which is used to lower the Free Fatty Acids (FFA) level in jatropha oil. The jatropha crude oil is heated to a temperature of 50°C, and then 13% methyl alcohol and 0.5% sulfuric acid are added to the heated oil. An excessive amount of methyl alcohol is added to quick the process. The reaction was conducted for 90 minutes at a temperature between 55 and 57 °C while being stirred at 700 rpm, with FFA analysis continuing every few minutes. As soon as the FFA content reaches 1%, the reaction stops. The fundamental problem with the acid-catalyzed esterification of FFA is the formation of water. The presence of water can slow down the conversion of FFA to esters. After being dewatered, the esterified oil was added to the transesterification procedure.

Sodium Hydroxide (NaOH) is a popular catalyst used in the trans-esterification process, contributing 1% of the total mass of the oil. It is distilled in 13% of distilled methanol (CH₃OH) using the standard agitator for 20 minutes at 700 rpm. Freshly prepared alcohol-catalyst solution was used to maintain catalytic activity and prevent moisture absorption. After completion, it is gradually charged into hot esterified oil. When methoxide is introduced to esterified oil, the system is closed to prevent moisture and alcohol loss. The reaction mixture was stirred at a speed of 560-700 rpm for 70 minutes while being kept at a temperature range of 60-65 °C (around the boiling point of methyl alcohol) to speed up the reaction. The reaction mixture was sampled for FFA analysis every 20 minutes.

The heating was stopped when the methyl ester had formed, and the products were cooled before being moved

to a separating funnel. After the reaction is finished, it is allowed to settle for 8 to 10 hours in a separating funnel. At this moment, glycerin and biodiesel are the two main products that have been obtained. Due to its weight, the glycerin component has settled as opposed to the biodiesel component, which has risen. After the glycerin and biodiesel phases were separated, the surplus alcohol in each stage was removed by the distillation procedure. The produced jatropha biodiesel was refined by washing gently with warm water to remove any leftover catalysts or soaps after the glycerin and alcohol were removed.

Jatropha biodiesel is denoted as JB, followed by a number indicating the proportion. The experiment was executed with different volumes of Jatropha biodiesel, each having 10, 20, and 30% JB methyl ester. It signifies that JB10D90 includes 10% Jatropha Methyl Ester (JME) and 90% Pure Diesel, JB20D80 contains 20% JME and 80% Standard Diesel, and JB30D70 contains 30% JME and 70% Diesel.

The density of the biodiesel and its blends was determined as per ASTM D-287 standard at 15°C. The measurement has been performed using a hydrometer instrument. According to ASTM D93-58T standards, the flash and fire points of samples were characterized with the help of the Pensky-Martin apparatus which heated and stirred at a constant rate. The instrument Red-Wood Viscometer was used to measure the viscosity of jatropha biodiesel with its blends at 40°C as per ASTM D445 standard. With the help of an ignition quality tester, the cetane number was measured according to ASTM D613 standards. The calorific value of the biodiesel was

Table 1. Properties of diesel-biodiesel blends

Properties	Diesel	Jatropha biodiesel	JB10D90	JB20D80	JB30D70	ASTM Standard
Density (Kg/m ³)	830	998	885	904	966	ASTM D287
Flashpoint(°C)	53	84	64	70	79	ASTM D93-58T
Viscosity@40°C(cSt)	2.09	10.8	2.92	3.19	4.02	ASTM D445
Cetane number	49	43	48	47	45	ASTM D613
Firepoint(°C)	56	102	75	81	94	ASTM D93-58T
Calorific Value (KJ/Kg)	42991	37450	42276	41965	41802	ASTM D4809

determined at using a Bomb calorimeter according to ASTM D4809 standards.

2.2 Experimental Setup

The line diagram and image of the VCR engine is depicted in Figure 1 and Figure 2. The setup features a Kirloskar engine with a 5 bhp capacity, operating at 1500 rpm, and maintaining a compression ratio of 16.5. A crank angle

sensor on the flywheel monitors the rotation, while a pressure sensor on the cylinder head gauges in-cylinder pressure. Temperature sensors at specific engine locations measure air and cooling water temperatures. Engine load is digitally regulated using a 5hp eddy current dynamometer connected to the engine. Detailed specifications of this setup are provided in Table 2. For data acquisition during experiments, the system utilized IC Enginesoft_9.0 software. Additionally, emissions of

Table 2. Specifications of the experimental engine

Name of the Engine	Variable compression ratio with 1-cylinder, 4-stroke diesel engine
Engine maker	Kirloskar engine
Version and Power rated(bhp)	AV 1 and 3.7kW
Bore diameter	80mm
Speed	1500rpm
Actual compression ratio	16.5:1 VCR range 10:1 to 20:1
Actual fuel injection timing	23° BTDC
Opening the exhaust valve at	4.5° ATDC
Stroke	110mm
CC	0.553L
Dynamometer and rated power	Eddy Current and 5HP at 1500 RPM

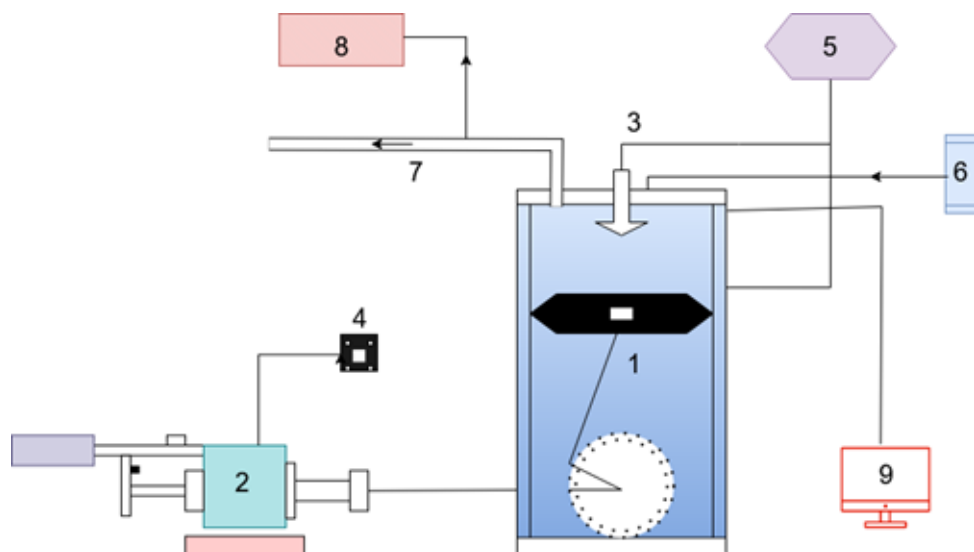


Figure 1. Schematic representation of engine test setup.

1. Kirloskar oil engine, 2. Dynamometer, 3. Injector, 4. Control Panel, 5. Fuel tank, 6. Air filter, 7. Exhaust gas silencer, 8. Exhaust gas analyzer, 9. Data acquisition system



Figure 2. Image of VCR engine.

Nitrogen Oxides (NO_x), Carbon Monoxide (CO), and Hydrocarbons (HC) were analyzed using the AVL DiGas 444 exhaust gas analyzer.

3.0 Results and Discussion

After obtaining the test data, a response analysis was performed using the input data, which included the Fuel Proportions (FP), Engine Load (L), and Compression Ratio (CR), and a quadratic process order was given to complete the study. Regression equations that demonstrate the correlation between the input and output parameters may often be expressed from Equations (1)-(5).

In Table 3, the p-values and coefficient determination of responses for the engine characteristics are presented. Interestingly, p-values (<0.0001) were observed for all analyses, indicating that the model was more effective in rejecting the null hypothesis. It might be noticed that R² was found to be greater than 0.98 for all responses,

resulting in a simpler regression line. Additionally, adjusted R² and predicted R² are probably compared with previous works⁴⁰. The analyses and computations presented in this research were conducted using Design expert software with version 12.

3.1 Performance of Engine

3.1.1 Brake Thermal Efficiency (BTE)

In Figure 3 BTE might be shown modified input data. As seen in Figure, BTE increased along with load and CR for all blends. As a result of higher L and higher CR, which encouraged to get higher temperature and pressure inside the cylinder and improved spray characteristics and the inception of a homogeneous air-fuel mixture, these results may be the reason for more complete and better fuel combustion inside the combustion chamber²²⁻²⁴. However, increasing the biodiesel mixing ratio in fuel mixes was found to have a negative effect on BTE. Evidently, the lower

Table 3. Coefficient determination and p-values

Model	BTE	BSFC	HC	CO	NO _x
R ²	0.9927	0.9878	0.9920	0.9999	0.9820
Adjusted R ²	0.9748	0.9670	0.9840	0.9683	0.9643
Predicted R ²	0.9628	0.9511	0.9832	0.9362	0.9343
p-value	<0.0001	<0.0001	<0.0001	<0.0001	<0.0001

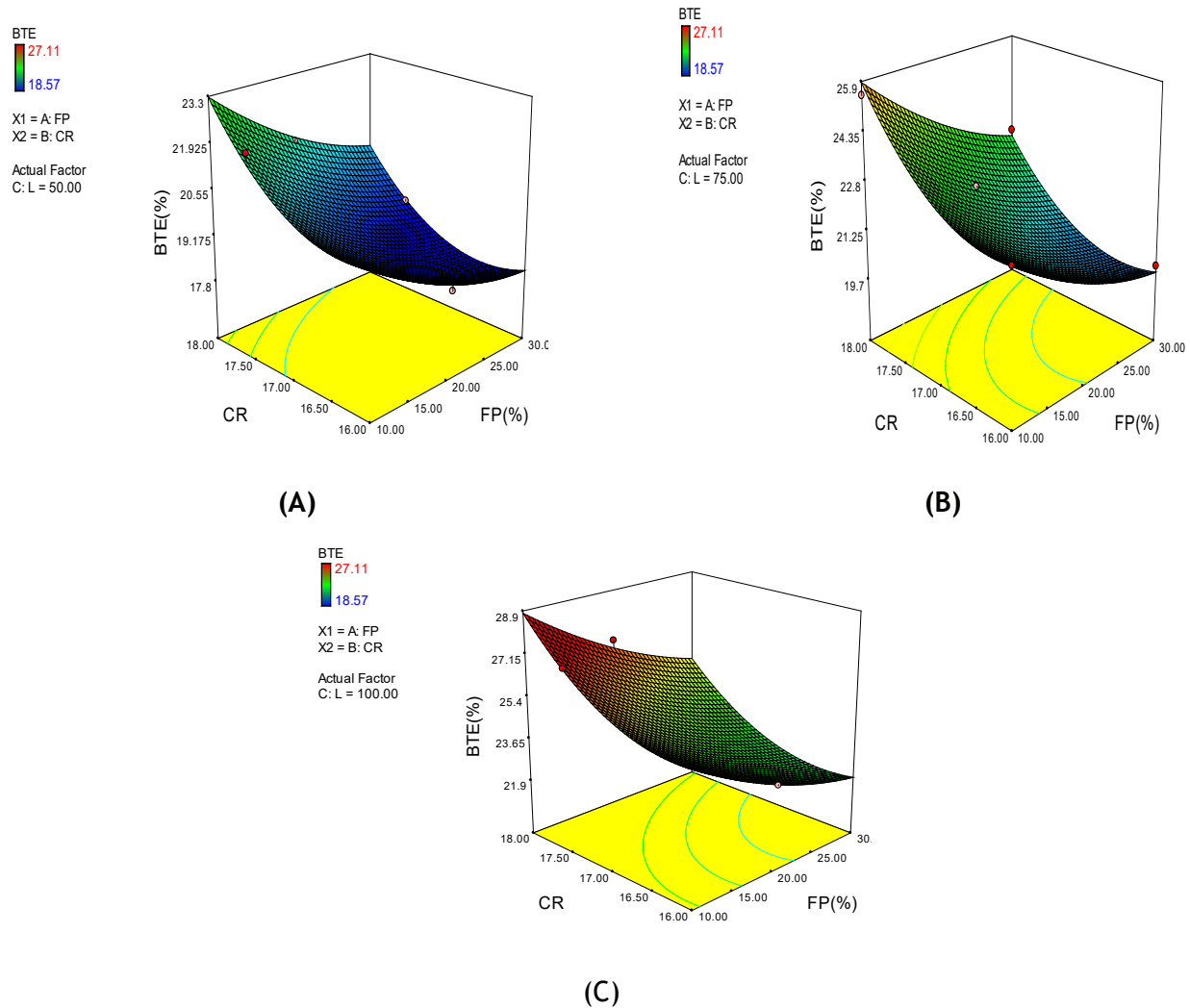


Figure 3. Correlation between BTE with input data. (A) Fuel proportions and CR at 50% load. (B) Fuel proportions and CR at 75% load. (C) Fuel proportions and CR at 100% load.

heating value of biodiesel could result in a lesser heating value being produced during combustion than diesel fuel^{25,26}. Additionally, increasing the amount of biofuel in blends could result in an increase in the land surface tension kinematic viscosity of the fuel blends, which would lead to poor evaporation and atomization^{27,28}. In Figure 3, the highest BTE of 28.63% could be noticed at CR = 18, L = 100%, and FP = 10% biodiesel/90% diesel. In contrast, the lowest BTE 17.48% was observed at CR = 16, L = 50%, and FP = 30% biodiesel/70% diesel fuel.

$$\begin{aligned}
 \text{BTE} = & 312.27292 + 0.087417 * \text{FP} - 35.84736 * \text{CR} - 0.053633 \\
 & * \text{L} - 0.020611 * \text{FP} * \text{CR} - 8.60000\text{E} - 0.44 * \text{FP} * \text{L} \\
 & + 7.28889\text{E} - 00. * \text{CR} * \text{L} + 4.46250\text{E} - 003 * \text{FP}^2 + \\
 & 1.09417 * \text{CR}^2 + 2.78000\text{E} - 004 * \text{L}^2 \quad (1)
 \end{aligned}$$

3.1.2 Brake-Specific Fuel Consumption (BSFC)

Figure 4 might show the outcomes of the BSFC employing RSM with respect to FP, L, and CR. Figure shows a conflicting trend of BSFC in contrast to BTE for all of the test engine's input data. With rising FP, there was undoubtedly a rise in BSFC, and using all blends of fuel for the test engine revealed a negative trend for load and CR as well²⁹. For internal combustion engines, bio-fuel has a lower heating value and higher kinematic viscosity than diesel fuel, which has increased the quantity of fuel injected inside the combustion chamber. This is because diesel engine fuel injection is a constant volume operation^{30,31}. In Figure 4, the BSFC is 0.59 kg/kWh at

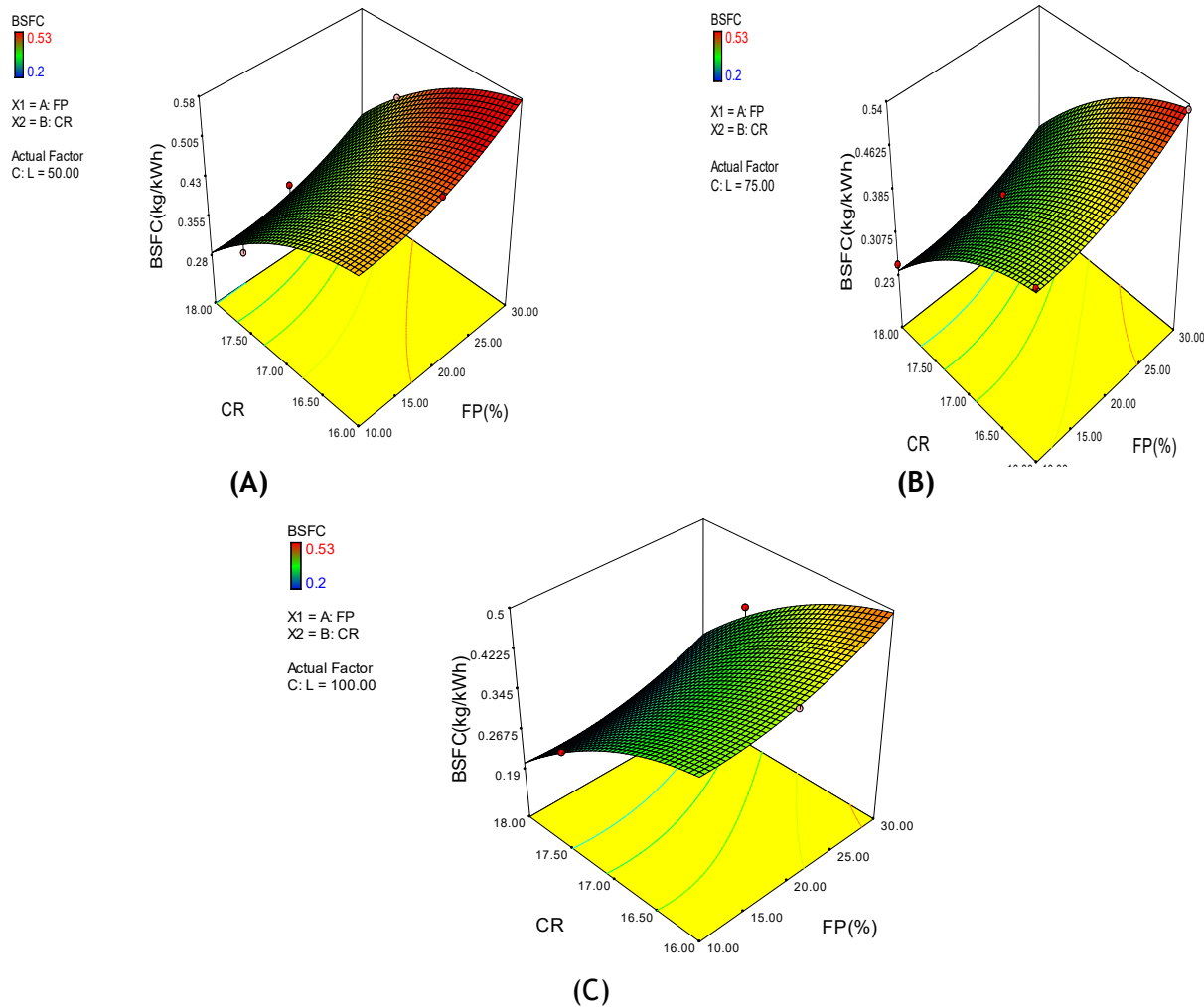


Figure 4. Correlation between BSFC with input data. (A) Fuel proportions and CR at 50% load. (B) Fuel proportions and CR at 75% load. (C) Fuel proportions and CR at 100% load.

CR = 16:1, FP = 30%biodiesel/70%diesel, and L = 50%, which is higher than BSFC attained at CR = 18:1; FP = 10%biodiesel/90%diesel fuel and 100% L. These findings could be explained by the higher CR promoting fuel atomization, resulting in improved fuel particles. On the other hand, increasing CR in permutation with higher load (L) could raise temperature and pressure inside the cylinder, improving combustion and significantly lowering brake-specific fuel consumption.

$$\begin{aligned}
 \text{BSFC} = & -8.30417 + 5.33333\text{E-}003 * \text{FP} + 1.11528 * \text{CR} + 1.333 \\
 & 33\text{E} - 003 * \text{L} - 5.55556\text{E-}004 * \text{FP} * \text{CR} - 2.00000\text{E-} \\
 & 005 * \text{FP} * \text{L} - 2.22222\text{E-}004 * \text{CR} * \text{L} + 2.50000\text{E-} 004 \\
 & * \text{FP}^2 - 0.035000 * \text{CR}^2 + 8.00000\text{E-}006 * \text{L}^2
 \end{aligned}
 \tag{2}$$

3.2 Emission parameters

3.2.1 Unburnt Hydrocarbon (HC)

As shown in Figure 5, the correlation between HC emissions and changes in CR, FP, and L could be seen, there was a rise in HC emissions as L increased, while HC emissions decreased as FP and CR increased. Increasing the biodiesel concentration in proportions might be the primary factor for falling the amount of HC emissions because biodiesel made from jatropha, which contains oxygen, is known to increase oxidation during the combustion process³². As the CR was increased, however, the spray of the fuel and the creation of the air-fuel mixture were also enhanced, which improved fuel

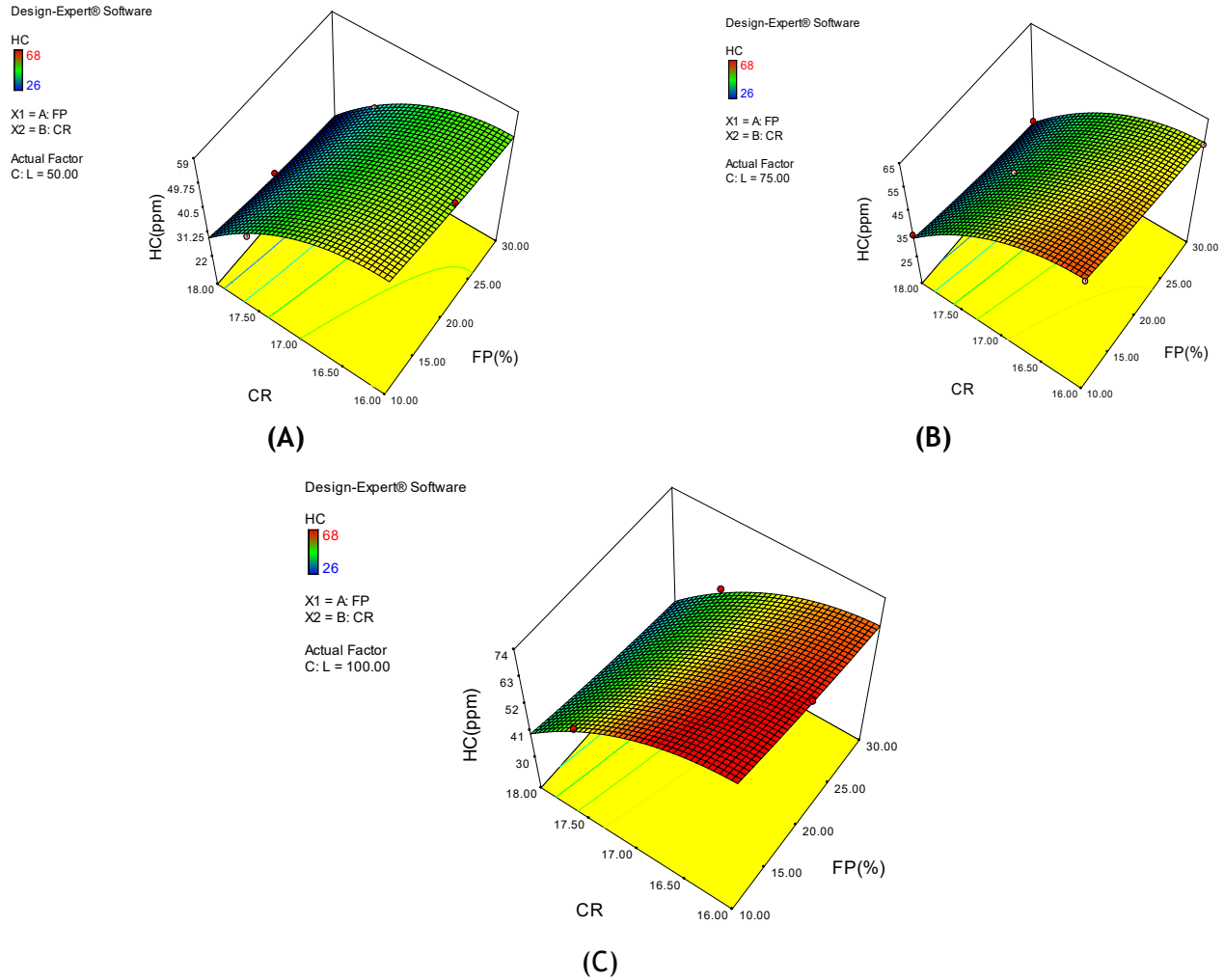


Figure 5. Correlation between HC emissions with input data. (A) Fuel proportions and CR at 50% load. (B) Fuel proportions and CR at 75% load. (C) Fuel proportions and CR at 100% load.

combustion and oxidation in the cylinder. As a result, increasing CR may be seen of as a way to effectively reduce HC emissions. This finding might help to explain that petrol engines with low CR release higher emissions of HC than diesel engines⁴⁵. In Figure 5, the maximum HC emissions 71 ppm could be noticed at CR16, FP 10% biodiesel/90%diesel and 100% load. On the other hand, the lower HC emissions 24 ppm also be recorded in Figure 4 at CR18, FP 30% biodiesel/70%diesel and 50% load respectively.

$$\begin{aligned}
 \text{HC} = & -1884.79167 - 0.81667 * \text{FP} + 240.06944 * \text{CR} \\
 & + 0.80000 * \text{L} + 0.011111 * \text{FP} * \text{CR} - 2.00000\text{E} \\
 & - 003 * \text{FP} * \text{L} - 0.046667 * \text{CR} * \text{L} + 8.75000\text{E} - \\
 & 003 * \text{FP}^2 - 7.41667 * \text{CR}^2 + 1.80000\text{E} - 003 * \text{L}^2
 \end{aligned}
 \tag{3}$$

3.2.2 Carbon Monoxide

The fluctuation of CO emission in connection to CR, L, and FP could be deduced from the surface graphs shown in Figure 6. From the figure, it is clear that CO emissions rise sharply as L increases while falling when FP and CR rise. Certainly, the lowest emissions of CO 0.01%vol recorded at 50% load with 18 compression ratio and FP = 30%biodiesel/70%diesel. However, CO ramped up to 0.23% vol when CR16:1, L 100%, and FP 10%biodiesel/90%diesel. This outcome might be the consequence of a fuel-rich mixture being created by raising the load and injecting more fuel into the cylinder, which would lead to poor combustion and a rise in emissions of CO³⁶. However, raising CR was thought

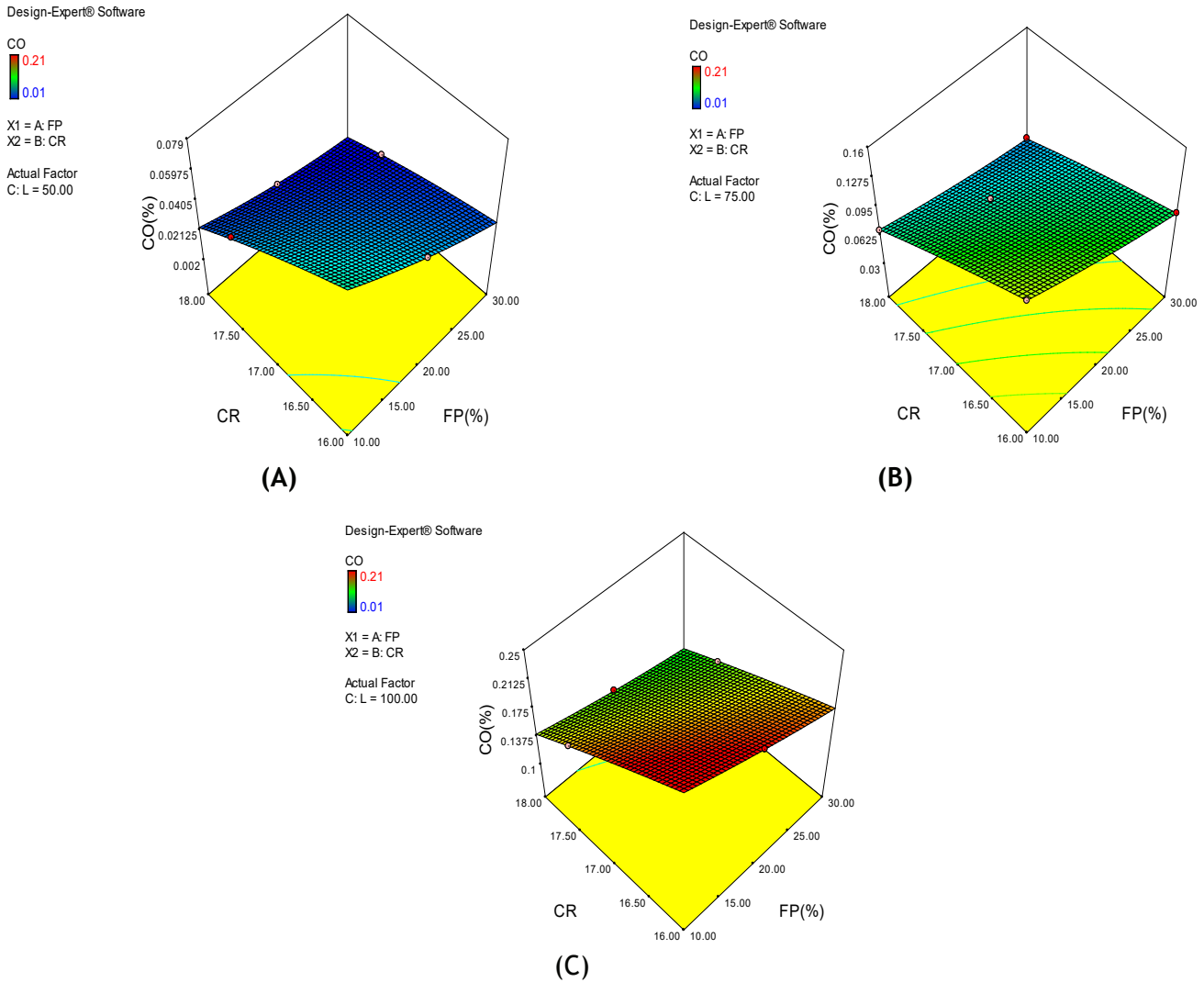


Figure 6. Correlation between CO emissions with input data. (A) Fuel proportions and CR at 50% load. (B) Fuel proportions and CR at 75% load. (C) Fuel proportions and CR at 100% load.

to increase cylinder pressure, resulting in improved homogenous and fine fuel-air mixture creation. The fuel burns more thoroughly as a result, producing more CO₂ and less CO emissions. The process that turns CO into CO₂ might potentially be facilitated by raising the oxygen content while also increasing the biofuel blending ratio.

$$CO = -0.31083 - 0.014083*FP + 0.048056*CR + 8.76667E-003 * L + 7.22222E - 004 * FP * CR - 2.00000E- 005 * FP * L - 5.11111E-004*CR*L + 2.50000E - 005 * FP^2 - 1.66667E- 003*CR^2+2.00000E- 005*L^2 \tag{4}$$

3.2.3 Oxides of Nitrogen (NOx)

Figure 7 shows the correlation between the trend change in NOx emissions and the FP ratios, CR, and L. It was evident that raising all three input values led to an increase in NOx emissions. The relationship between engine load and compression ratio could be elucidated by the possibility that increased load and CR could raise the combustion chamber’s temperature and facilitate the separation of the nitrogen molecules into N atoms furthermore the effect between oxygen and N atoms produces nitrogen oxide emissions³³. The greater temperature and pressure

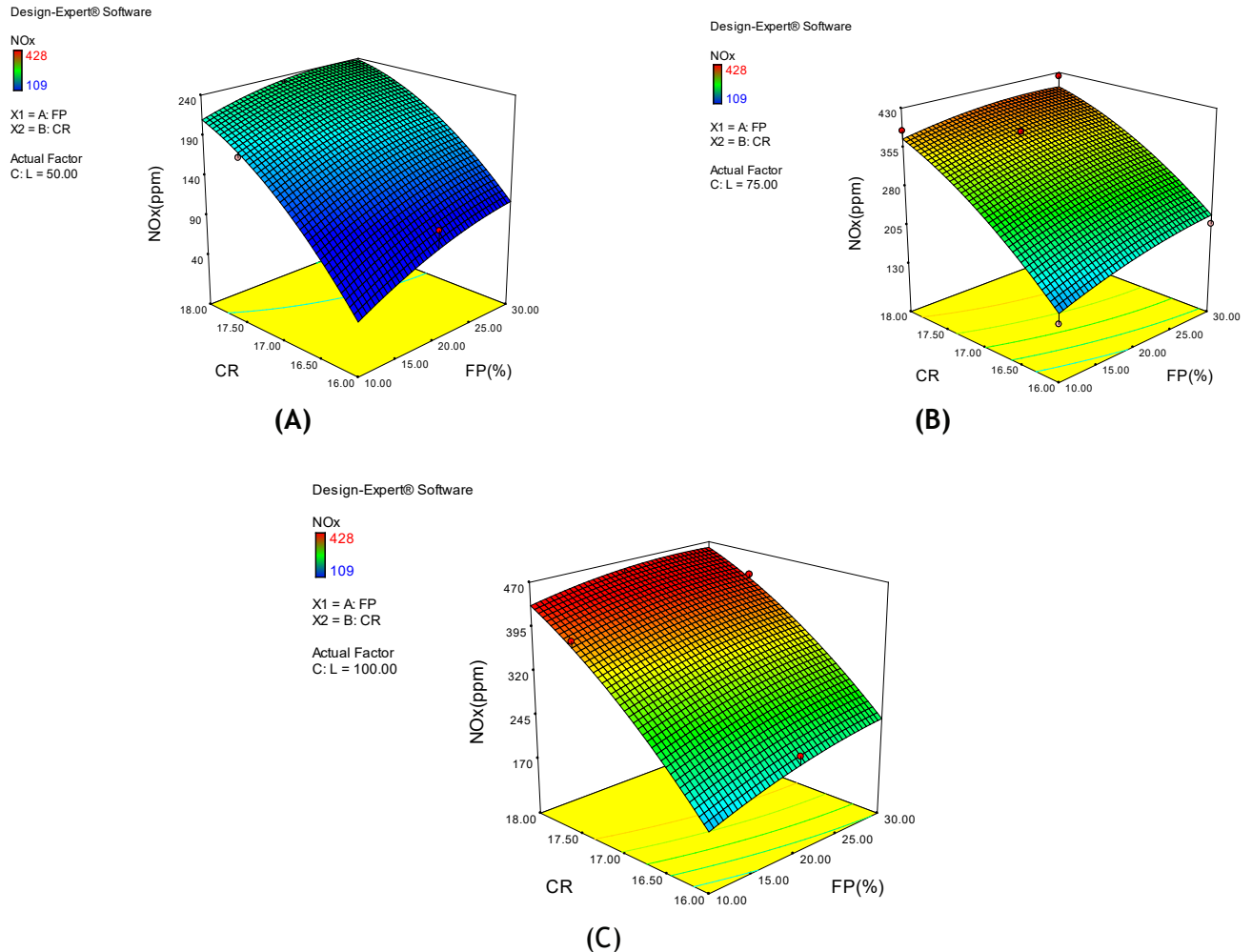


Figure 7. Correlation between emissions of NOx with input data. (A) Fuel proportions and CR at 50% load. (B) Fuel proportions and CR at 75% load. (C) Fuel proportions and CR at 100% load.

at higher CR might potentially result in much higher NOx emissions at the same load than at lower CR. When the amount of bio-oil in fuel blends was raised for the vary in FP, the oxygen concentration increased as well, which gave more time to create the air-fuel combination and lengthened the ignite delay³⁴. Better combustion of the air-fuel combination as a result rises the chamber temperature and increases NOx emissions³⁵. From Figure 7, it can be noticed that the highest emissions of NOx 466 ppm observed for FP = 30%biodiesel/70%diesel and CR = 18:1 with 100% load whereas the lowest amount of NOx could be noticed at 16:1CR, 50% load, and FP = 10%biodiesel/90%diesel.

$$\text{NOx} = 7933.58333 + 24.29167 \cdot \text{FP} + 825.63889 \cdot \text{CR} + 0.35000 \cdot \text{L} - 1.02778 \cdot \text{FP} \cdot \text{CR} + 0.000000 \cdot \text{FP} \cdot \text{L} + 0.91333 \cdot \text{CR} \cdot \text{L} - 0.11000 \cdot \text{FP}^2 - 22.83333 \cdot \text{CR}^2 - 0.082400 \cdot \text{L}^2 \quad (5)$$

The performance and emission characteristics discussed above show that increasing the compression ratio causes BTE, NOx to trend downward while the rest of the responses trend upward. The BTE, NOx, CO, and HC also increase as engine load increases, although BSFC decreases. Additionally, an increase in blend results in an increase in BSFC and NOx and a decrease in the other responses. It is clear that these three input factors influence the output responses differently. In

Table 4. Optimizing process measure

I/P and O/P data	Unit	Range	weight	Importance	criteria
CR		16-18	1	1	Within range
L	%	50-100	1	1	
FP	%	10-20	1	1	
BTE	%	17.48-28.63	1	1	Max.
BSFC	%	0.2-0.59	1	1	Min.
HC	ppm	24-71	1	1	
CO	%	0.01-0.23	1	1	
NOx	ppm	104-466	1	1	

Table 5. Validation of experiments

Optimize parameters			Values	Performance		Emissions		
				BTE (%)	BSFC (kg/kW)	HC (ppm)	CO (%)	NOx (ppm)
FP(%)	L%	CR						
10%biodiesel, 90%diesel	50	18:1	Predicted	23.186	0.285	36	0.024	224
			Actual	23.258	0.306	38	0.026	216
			Error (%)	-0.61	-3.65	-2.3	-2.91	2.18

order to improve efficiency and significantly reduce emission levels, it is vital to identify ways to optimize the input conditions. Table 4 shows a possible aim for the answers to obtain optimum input data. It is possible to maximize BTE while minimizing BSFC, NOX, HC, and CO. The optimal input parameters are determined to be a fuel mix containing 10% biodiesel, a load of 50% with a compression ratio of 18:1, and a desirability factor of 0.615. The engine's optimal input parameters were determined to be 18:1 CR, FP = 10% biodiesel/90% diesel, and L = 50%.

As a result, these input parameters are specified, and the test is repeated three times. The collected findings are averaged and reported in Table 5, where the percentage error is less than 5%, indicating a satisfactory agreement between tested and expected values^{36,37}.

4.0 Conclusions

In this experiment, the compression ratio was varied from 16 to 18, at different loads 50, 75 and 100%, and the biodiesel blending ratio was 10%, 20%, and 30% in diesel respectively. In general, the following findings might be withdrawn:

- The highest BTE 28.63% was noticed at CR 18:1 with 100% load and biodiesel blend of 10% jatropha biodiesel and 90% diesel. Similarly, the test engine showed the lowest BSFC of 0.2 kg/kWh when it was run at an engine load of 100% with 18:1 CR, and a blend of 10% biodiesel, 90% diesel.
- With increase an in engine load and reduction in the biodiesel blending proportion in diesel and

compression ratio, results in a decrease in the HC and CO emissions. As a consequence, the maximum CO and HC emissions were 0.23% and 71 ppm respectively, at 16:1 CR with 100% engine load and 10% biodiesel, 90% diesel. However, in the best operating conditions, CO and HC emissions be the lowest, equivalent to 0.01 percent and 24 ppm respectively.

- NO_x emissions increased as compression ratio, engine load, and biodiesel-diesel fuel mixing ratio increased. From outcomes, the highest NO_x emission 466ppm was recorded at 18:1 CR with 100% load and blended ratio of 30% biodiesel/70% diesel. At 50% load, 16:1 CR, and 10% biodiesel, 90% diesel blend produced the lowest NO_x emission, which was recorded at 104 ppm.

In summary, the application of RSM for engine parameter optimization might provide a desirable method in which BTE could reach the highest values, while BSFC and the other emission characteristics were kept to a minimum. The use of 10% biodiesel blended with 90% pure diesel in combination with a 50% load at 18:1CR could be regarded as an optimized operation condition for the test set-up with 0.615 desirability factor and <5% error for verified parameters formulated on the results of the RSM estimation

5.0 References

1. Khan HM, Ali CH, Iqbal T, Yasin S, Sulaiman M, Mahmood. Current scenario and potential of biodiesel production from waste cooking oil in Pakistan: An overview. *Chin J Chem Eng.* 2018; 27(10):2238-50.
2. Das S, Kashyap D, Kalita P, Kulkarni V, Itaya Y. Clean gaseous fuel application in diesel engine: A sustainable option for rural electrification in India. *Renew Sust Energ Rev.* 2020; 117:109485. <https://doi.org/10.1016/j.rser.2019.109485>
3. Soudagar MEM, Nik-Ghazali NN, Kalam MA, Badruddin IA, Banapurmath NR, Akram N. The effect of nano-additives in diesel-biodiesel fuel blends: A Comprehensive review on stability, engine performance, and emission characteristics. *Energy Conv Manag.* 2018; 178:146-77. <https://doi.org/10.1016/j.enconman.2018.10.019>
4. Pan H, Li H, Zhang H, Wang A, Jin D, Yang S. Effective production of biodiesel from non-edible oil using a facile synthesis of imidazolium salts-based Brønsted-Lewis solid acid and co-solvent. *Energy Conv Manag.* 2018; 166:534-44. <https://doi.org/10.1016/j.enconman.2018.04.061>
5. Quah RV, Tan YH, Mubarak NM, Khalid M, Abdullah EC, Nolasco-Hipolito C. An overview of biodiesel production using recyclable biomass and non-biomass derived magnetic catalysts. *J Environ Chem Eng.* 2019; 103219.
6. Rajak U, Verma TN. Effect of emission from ethylic biodiesel of edible and Non-edible vegetable oil, animal fats, waste oil, and alcohol in CI engine. *Energy Conv Manag.* 2018; 166:704-18.
7. Nour M, Attia AM, Nada SA. Combustion, performance, and emission analysis of diesel engine fuelled by higher alcohols (butanol, octanol, and heptanol)/diesel blends. *Energy Conv Manag.* 2019; 185:313-29. <https://doi.org/10.1016/j.enconman.2019.01.105>
8. Nanthagopal K, Ashok B, Garnepudi RS, Tarun KR, Dhinesh B. Investigation on diethyl ether as an additive with *Calophyllum inophyllum* biodiesel for CI engine application. *Energy Conv Manag.* 2019; 179:104-13. <https://doi.org/10.1016/j.enconman.2018.10.064>
9. Hirner FS, Hwang J, Bae C, Patel C, Gupta T, Agarwal AK. Performance and Emission evaluation of a small-bore biodiesel compression-ignition engine. *Energy.* 2019; 183:971-82.
10. Singh D, Sharma D, Soni SL, Sharma S, Kumari D. Chemical compositions, Properties and standards for different generation biodiesels: A review fuel. 2019; 253:60-71. <https://doi.org/10.1016/j.fuel.2019.04.174>
11. Gülüm M, Bilgin A. A comprehensive study on measurement and prediction of viscosity of biodiesel-diesel-alcohol ternary blends. *Energy.* 2018; 148:341-61. <https://doi.org/10.1016/j.energy.2018.01.123>
12. Noor CM, Noor MM, Mamat R. Biodiesel as an alternative fuel for marine diesel Engine applications: A review. *Renew Sustain Energ Rev.* 2018; 94:127-42.
13. Keskin A. The effect of cottonseed oil methyl ester-euro diesel fuel blends on the combustion, performance, and emission characteristics of a direct injection diesel engine. *J Fac Eng Archit.* 2019; 34(2):916-27. <https://doi.org/10.1093/arclin/acz034.56>
14. Pathak A, Choudhury PK, Dutta RK. Taguchi-Grey relational-based multi-objective optimization of process parameters on the emission and fuel consumption characteristics of a VCR petrol engine. *Mater Today: Proc.* 2018; 5(2):4702-10. <https://doi.org/10.1016/j.matpr.2017.12.042>

15. Esonye C, Onukwuli OD, Ofoefule AU. Optimization of methyl ester production from *Prunus amygdalus* seed oil using response surface methodology and artificial neural networks. *Renew Energy*. 2019; 130:61-72. <https://doi.org/10.1016/j.renene.2018.06.036>
16. Krishnamurthy KN, Sridhara SN, Ananda Kumar CS. Synthesis and optimization of *Hydnocarpus wightiana* and dairy waste scum as feedstock for biodiesel production by using response surface methodology. *Energy*. 2018; 153:1073-86. <https://doi.org/10.1016/j.energy.2018.04.068>
17. Singh Y, Singh P, Sharma A, Choudhary P, Singla A. Optimization of wear and friction characteristics of *Phyllanthus emblica* seed oil-based lubricant using response surface methodology. *Egypt J Pet*. 2018; 27(4):1145-55. [https://doi.org/10.1053/S1557-5063\(18\)30191-5](https://doi.org/10.1053/S1557-5063(18)30191-5)
18. Yusri IM, Abdul Majeed APP, Mamat R, Ghazali MF, Awad OI, Azmi WH. A review on the application of response surface method and artificial neural network in engine performance and exhaust emissions characteristics in alternative fuel. *Renew Sustain Energy Rev*. 2018; 90:665-86.
19. Kumar D, Singh B. *Tinospora cordifolia* stem extract as an antioxidant additive for enhanced stability of Karanja biodiesel. *Ind Crops Prod*. 2018; 123:10-6. <https://doi.org/10.1016/j.indcrop.2018.06.049>
20. Kumar S, Dinesha P. Optimization of engine parameters in a biodiesel engine run with honge methyl ester using response surface methodology. *Measurement*. 2018; 125:224-31. <https://doi.org/10.1016/j.measurement.2018.04.091>
21. Yatish KV, Lalith Amba HS, Suresh R, Harsha Hebbar HR. Optimization of *bauhinia variegata* biodiesel production and its performance, combustion, and emission study on diesel engine. *Renew Energy*. 2018; 122:561-75. <https://doi.org/10.1016/j.renene.2018.01.124>
22. Rajamohan S, Kasimani R, Sadasivuni KK. Prediction of performance and emission characteristics of diesel engine fuelled with waste biomass pyrolysis oil using response surface methodology. *Renew Energy*. 2018; 136:91-103. <https://doi.org/10.1016/j.renene.2018.12.109>
23. Nayak SK, Nižetić S, Pham VV, Huang Z, Ölçer AI, Bui VG, Wattanavichien K, Hoang AT. Influence of injection timing on performance and combustion characteristics of compression ignition engine working on quaternary blends of diesel fuel, mixed biodiesel, and t-butyl peroxide. *J Clean Prod*. 2022; 333:130160. <https://doi.org/10.1016/j.jclepro.2021.130160>
24. Atarod P, Khlaife E, Aghbashlo M, Tabatabaei M, Hoang AT, Mobli H, Nadian MH. Soft computing-based modeling and emission control/reduction of a diesel engine fueled with carbon nanoparticle-dosed water/diesel emulsion of fuel. *J Hazard Mater*. 2021; 407:124369. <https://doi.org/10.1016/j.jhazmat.2020.124369>
25. Karagoz M, Uysal C, Agbulut U, Saridemir S. Energy, exergy, economic and sustainability assessments of a compression ignition diesel engine fueled with tire pyrolytic oil–diesel blends. *J Clean Prod*. 2020; 264:121724. <https://doi.org/10.1016/j.jclepro.2020.121724>
26. Hoang AT, Le AT and Pham VV. A core correlation of spray characteristics, deposit formation, and combustion of a high-speed diesel engine fueled with *Jatropha* oil and diesel fuel. *Fuel*. 2019; 244:159-75. <https://doi.org/10.1016/j.fuel.2019.02.009>
27. Ağbulut Ü, Karagöz M, Sarıdemir S, Öztürk A. Impact of various metal-oxide based nanoparticles and biodiesel blends on the combustion, performance, emission, vibration and noise characteristics of a CI engine. *Fuel*. 2020; 270:117521. <https://doi.org/10.1016/j.fuel.2020.117521>
28. Hoang AT. Experimental study on spray and emission characteristics of a diesel engine fueled with preheated bio-oils and diesel fuel. *Energy*. 2020; 171:795-808. <https://doi.org/10.1016/j.energy.2019.01.076>
29. Rajak U, Panchal M, Veza I, Ağbulut Ü, Verma T, Saridemir S, Shende V. Experimental investigation of performance, combustion and emission characteristics of a variable compression ratio engine using low-density plastic pyrolyzed oil and diesel fuel blends. *Fuel*. 2022; 319:123720. <https://doi.org/10.1016/j.fuel.2022.123720>
30. Hoang A, Pham M. Influences of heating temperatures on physical properties, spray characteristics of bio-oils and fuel supply system of a conventional diesel engine. *Int J Adv Sci Eng Inf Technol*. 2018; 8:2231-40.
31. Hoang AT, Pham VV. Impact of *jatropha* oil on engine performance, emission characteristics, deposit formation, and lubricating oil degradation. *Combust Sci Technol*. 2019; 191(3):504-19.
32. Jayaraman J, Alagu K, Appavu P, Joy N, Jayaram P, Mariadoss A. Enzymatic production of biodiesel using lipase catalyst and testing of an unmodified compression ignition engine using its blends with diesel. *Renew*

- Energy. 2020; 145:399-407. <https://doi.org/10.1016/j.renene.2019.06.061>
33. Varatharajan K, Cheralathan M. Influence of fuel properties and composition on NOx emissions from biodiesel powered diesel engines: A review. *Renewable and Sustainable Energy Reviews*. 2021; 16(6):3702-10.
 34. Hoang AT, Ölçer AI, Nižetić S. Prospective review on the application of biofuel 2, 5-dimethylfuran to diesel engine. *J Energy Inst*. 2021; 94:360-86. <https://doi.org/10.1016/j.joei.2020.10.004>
 35. Nayak SK, Hoang AT, Nayak B, Mishra PC. Influence of fish oil and waste cooking oil as post mixed binary biodiesel blends on performance improvement and emission reduction in a diesel engine. *Fuel*. 2021; 289:119948. <https://doi.org/10.1016/j.fuel.2020.119948>
 36. Sharma A, Murugan S. Potential for using a tyre pyrolysis oil-biodiesel blends in a diesel engine at different compression ratios. *Energy Conv Manag*. 2015; 93:289-97. <https://doi.org/10.1016/j.enconman.2015.01.023>
 37. Datta Bharadwaz Y, Govinda Rao B, Dharma Rao, V, Anusha C. Improvement of biodiesel methanol blends performance in a variable compression ratio engine using response surface methodology. *Alex Eng J*. 2016; 55(2):1201-09. <https://doi.org/10.1016/j.aej.2016.04.006>
 38. Sunil Kumar, Sumit Bansal. Performance evaluation of ANFIS and RSM in modeling biodiesel synthesis from soybean oil. *Biosensors and Bioelectronics: X*. 2023; 15:100408. <https://doi.org/10.1016/j.biosx.2023.100408>
 39. Pitchaiah. Prediction and performance optimization of a DI CI engine fueled diesel-Bael biodiesel blends with DMC additive using RSM and ANN: Energy and exergy analysis. *Energy Conversion and Management*. 2023; 292(15):117386. <https://doi.org/10.1016/j.enconman.2023.117386>
 40. Kumar V, Rajesh Kumar S. The effect of operating parameters on performance and emissions of DI diesel engine fuelled with Jatropha biodiesel. *Fuel*. 2020; 278(15):118256. <https://doi.org/10.1016/j.fuel.2020.118256>

List of Abbreviations

RSM	Response surface methodology
BTE	Brake Thermal Efficiency (%)
BSFC	Brake specific fuel consumption (kg/kWh)
HC	Hydrocarbon
CO	Carbon monoxide
CO ₂	Carbon dioxide
NOx	Oxides of nitrogen
ASTM	American Society for Testing and Materials
FP	Fuel proportions
CR	Compression ratio
L	Load
CI	Compression Ignition
JB10D90	10% Jatropha, 90% diesel
JB20D80	20% Jatropha, 80% diesel
JB30D70	30% Jatropha, 70% diesel
FAME	Fatty acid methyl ester
FFA	Free fatty acid
VCR	Variable compression ratio